

## RESEARCH ARTICLE

# Molecular mechanisms involved in drug-induced liver injury caused by urate-lowering Chinese herbs: A network pharmacology study and biology experiments

Fan Li<sup>☉</sup>, Yi-Zhu Dong<sup>☉</sup>, Dan Zhang, Xiao-Meng Zhang, Zhi-Jian Lin, Bing Zhang<sup>✉</sup>\*

Department of Clinical Chinese Pharmacy, School of Chinese Materia Medica, Beijing University of Chinese Medicine, Chao Yang District, Beijing, China

☉ These authors contributed equally to this work.

\* [zhangb@bucm.edu.cn](mailto:zhangb@bucm.edu.cn)



## OPEN ACCESS

**Citation:** Li F, Dong Y-Z, Zhang D, Zhang X-M, Lin Z-J, Zhang B (2019) Molecular mechanisms involved in drug-induced liver injury caused by urate-lowering Chinese herbs: A network pharmacology study and biology experiments. PLoS ONE 14(5): e0216948. <https://doi.org/10.1371/journal.pone.0216948>

**Editor:** Manas Ranjan Dikhit, Rajendra Memorial Research Institute of Medical Sciences, INDIA

**Received:** February 17, 2019

**Accepted:** May 1, 2019

**Published:** May 29, 2019

**Copyright:** © 2019 Li et al. This is an open access article distributed under the terms of the [Creative Commons Attribution License](https://creativecommons.org/licenses/by/4.0/), which permits unrestricted use, distribution, and reproduction in any medium, provided the original author and source are credited.

**Data Availability Statement:** All relevant data are within the manuscript and its Supporting Information files.

**Funding:** The funder had no role in study design, data collection and analysis, decision to publish, or preparation of the manuscript.

**Competing interests:** The authors have declared that no competing interests exist.

## Abstract

As an important part of the comprehensive treatment methods, the urate-lowering Chinese herbs could provide favorable clinical effects on hyperuricemia in its ability to invigorate spleen and remove dampness. Owing to the long-term duration, it brought up the potential adverse reactions (ADRs) and concerns about the drug-induced liver injury from these herbs. To address this problem, the bioinformatics approaches which combined the network pharmacology, computer simulation and molecular biology experiments were undertaken to elucidate the underlying drug-induced liver injury molecular mechanisms of urate-lowering Chinese herbs. Several electronic databases were searched to identify the potential liver injury compounds in published research. Then, the putative target profile of liver injury was predicted, and the interaction network was constructed based on the links between the compounds, corresponding targets and core pathways. Accordingly, the molecular docking simulation was performed to recognize the representative compounds with hepatotoxicity. Finally, the cell experiments were conducted to investigate the biochemical indicators and expression of the crucial protein that were closely associated with liver injury. In conclusion, the current research revealed that the compounds with potential liver injury including diosgenin, baicalin, saikosaponin D, tetrandrine, rutaecarpine and evodiamine from urate-lowering Chinese herbs, could lead to decline the survival rate of L-02 cell, increase the activities of aspartate aminotransferase (AST), alanine aminotransferase (ALT), lactate dehydrogenase (LDH) and alkaline phosphatase (ALP) in cell-culture medium, enhance the expression of p-p38/p38, while the p38 inhibitor could achieve the trend of regulating and controlling liver injury. These research findings bring further support to the growing evidence that the mechanism of the liver injury induced by the compounds from urate-lowering Chinese herbs may be associated with the activation of p38 $\alpha$ .

## Introduction

Hyperuricemia is defined as a serum urate concentration exceeding the limit of solubility (approximately 6.8 mg/dl), is commonly considered as a metabolic abnormality that caused by the obstacles in purine metabolism or a decrease in the excretion of uric acid [1–3]. In view of the rapid economic development along with the diet and lifestyle changes, the prevalence of hyperuricemia has increased over 21% and 13% in the United States and Chinese general populations, respectively. Therefore, there has been an increasing trend in the prevalence of hyperuricemia, it becomes a serious public health problem worldwide currently [4–8]. Furthermore, hyperuricemia has been viewed as a clinically important risk factor for various diseases by numerous epidemiological studies, the higher level of serum uric acid are involved in metabolic syndrome (including hypertension, obesity, type 2 diabetes, dyslipidaemias, etc.), renal impairment (including chronic kidney disease, etc.), cardiac diseases (including coronary heart disease, heart failure and atrial fibrillation), stroke and peripheral arterial disease [9–13]. Recently, non-steroid anti-inflammatory drugs, benzbromarone, and allopurinol have a rapid onset for urate-lowering, making it a popular choice for the treatment of hyperuricemia [14–17]. Nevertheless, with the long-duration of hyperuricemia, these agents are associated with ADRs, for example, treatment with benzarone or benzbromarone may have the detrimental impact on hepatic injury [18]. And it is reported that allopurinol could cause hypersensitivity syndrome or Steven-Johnson syndrome in some cases [19].

To this relevant issue, traditional Chinese Medicine (TCM) has such advantages as multiple pathways, multi-targets to lower serum uric acid levels, and it has been extensively used in clinical practice for the thousands of years in Asian countries [20–21]. Theoretically speaking, Chinese herbs can exert the therapeutic effects of invigorating spleen and kidney, removing dampness and clearing away turbidness for regulating the uric acid metabolism; and it is regarded also as a considerable treatment by improving the metabolism of blood lipid abnormality and hepatorenal function [22–23]. Functionally, the candidate targets of TCM are significantly associated with several biological pathways by molecular biology techniques, such as regulating the mRNA and protein expressions of uric acid transporter and inhibiting the activity of xanthine oxidase [24–25]. However, given controlling the level of serum uric acid is a long-term process; therefore, it would also bring up the ADRs owing to the long duration of Chinese herbs. Recent pharmacological studies have declared that some herbal ingredients or compounds for treating hyperuricemia might improve the risk of ADRs, it is demonstrated that kaempferol and thymol in *Xiaochaihutang* and rhein in *Heshouwu* may be related to the potential liver injury targets [26–27]. With regard to the underlying drug-induced liver injury, the molecular mechanisms of urate-lowering Chinese herbs have not been fully elucidated due to the lack of appropriate research approaches. We performed the relative mechanism analysis via the approaches of network pharmacology, molecular docking simulation and cell experiments at the molecular level, which are the powerful tools based on contemporary in silico and in vitro methods to elucidate holistic and complex mechanisms of TCM with the rapid progress of bioinformatics, systems biology, and polypharmacology.

## Materials and methods

The current study was performed by four-step analysis, namely data preparation, network construction and analysis, molecular docking simulation and cell experiment in vitro. And the flowchart of the technical strategy was presented in Fig 1.

### Collection of potential drug-induced liver injury components in urate-lowering Chinese herbs

First, all kinds of studies concerning Chinese herbs that can induce drug-induced liver injury were selected by searching the following electronic databases up to May 2017: PubMed,

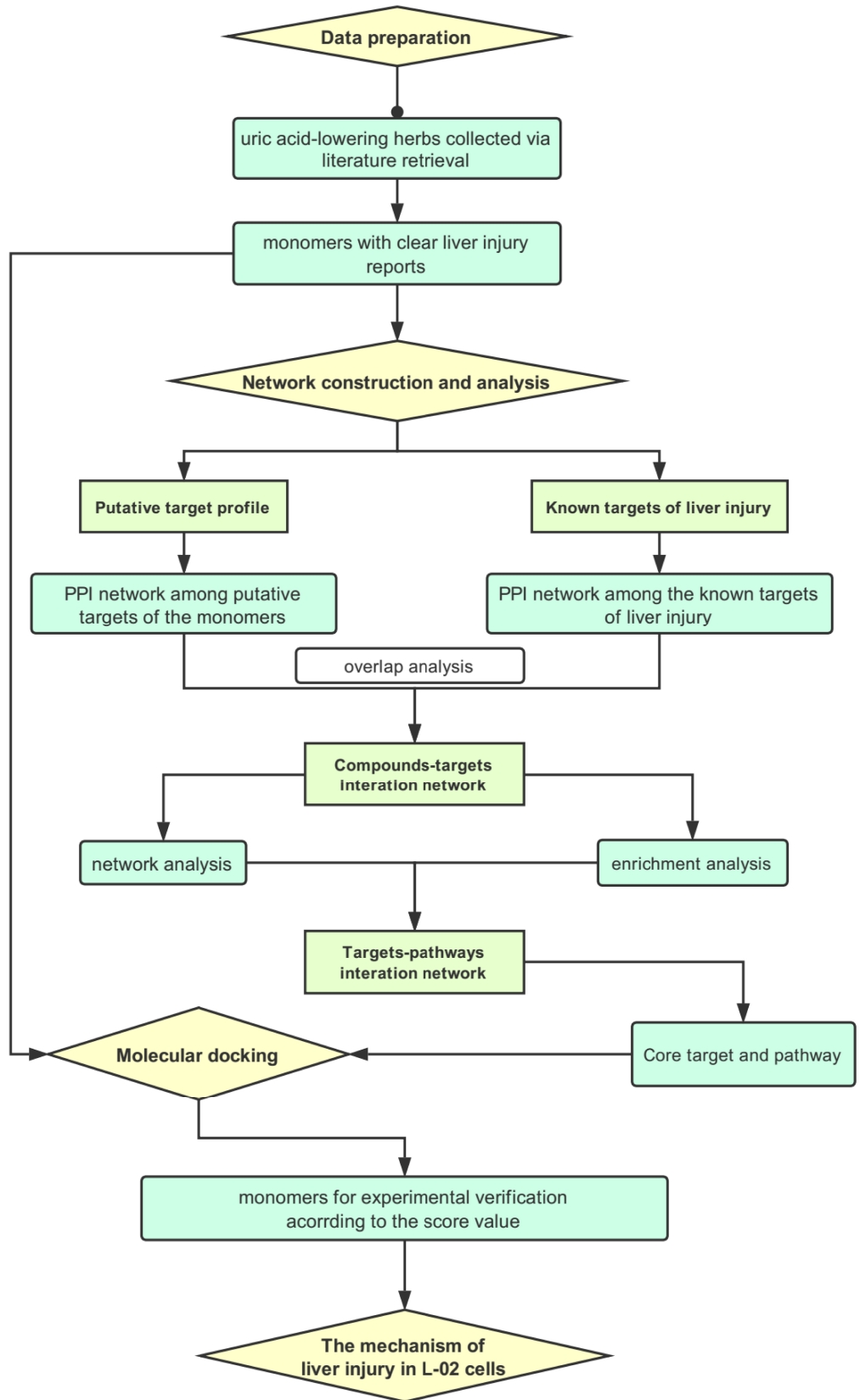


Fig 1. The flowchart of technical strategy in current study.

<https://doi.org/10.1371/journal.pone.0216948.g001>

Embase, Springer, the China National Knowledge Infrastructure Database (CNKI), the Wanfang Database, the Chinese Scientific Journals Full-text Database (VIP), and the Chinese Biomedical Literature Database (SinoMed). Moreover, according to the information of Chinese herbs that were recorded in the textbook of *Chinese Materia Medica* and Chinese pharmacopeia [28–29], the searching terms of Chinese herbs included the Decoction pieces name, Latin name, and *pinyin*. And the searching terms of drug-induced liver injury covered “adverse drug event\*”, “side effect\*”, “adverse drug reaction\*”, “drug toxicit\*”, “toxicity”, “toxic potential”, “liver injury”, “hepatotoxicity”, “liver damage”. Second, the literature with repetitive content, efficacy studies, the ADR of TCM formulas or Chinese patent medicine, and ADRs without liver injury was excluded via NoteExpress software. Through comprehensive collecting and combining the published literature of liver injury induced by urate-lowering Chinese herbs, the compounds or ingredients with potential liver injury from urate-lowering Chinese herbs were identified to build the database. Third, the Chem 3D package of molecular modeling software Chemoffice 2004 was utilized to depict the chemical and crystal structures, calculate various thermodynamic, electronic or steric parameters, and optimize molecular force field, ultimately, these data of components with potential liver injury was saved as mol 2 format [30–31].

### Prediction of putative liver injury targets

On the one hand, the related targets corresponding to the selected components were acquiring from traditional Chinese medicine systems pharmacology database and analysis platform (TCMSP) (<http://lsp.nwu.edu.cn/tcmsp.php>) and PharmMapper Database (<http://lilab.ecust.edu.cn/pharmmapper/>) [32–33]. It was noteworthy that TCMSP was developed as a digital repository of TCM, with more than 30,000 ingredients of Chinese herbs retrieved through literature mining and database integration [34]. In addition, Pharm Mapper Database was an online tool for drug-target identification via pharmacophore mapping approach [35]. During this procedure, “Human protein targets only (v2010, 2241)” was selected, besides, other parameters were set to default values, and the targets with  $z'$ -score > 0 of components with potential liver injury were chosen. The related targets from TCMSP and Pharm Mapper Database was in standard processing under the universal protein knowledgebase—UniProt (<https://www.uniprot.org/>) [36], the database of targets corresponding to the 32 candidate components with liver injury was built after identifying the redundant proteomes. On the other hand, the candidate target proteins relating to liver injury (keywords: “drug induce”, “drug-induced”, “drug-induced liver injury”, “drug-induced chronic hepatitis”, “liver injury, drug-induced”, “hepatitis, toxic”, “toxic liver disease”) were acquired in the Online Mendelian Inheritance in Man (OMIM) database (<http://www.omim.org/>, updated on April 21, 2016) [37], The Therapeutic Target (TTD) Database (<http://bidd.nus.edu.sg/group/cjttd/>, updated on Sep 10th, 2015) [38], the Pharmacogenomics Knowledgebase (PharmGKB) Database (<http://www.pharmgkb.org>) [39] and the Genetic Association Database (GAD) (<https://geneticassociationdb.nih.gov/>, updated on August 18, 2014) [40]. After removing redundant entries, the remaining proteins relating to liver injury were considered as candidate targets. Afterwards, the overlapping targets for the database of targets corresponding to the 32 candidate components from TCMSP and Pharm Mapper Database, and database of liver injury proteins from OMIM, TTD, PharmGKB, GAD were gathered as putative liver injury targets of 32 candidate components in current study for subsequent analyses.

### Protein-protein interaction (PPI) data

Further, to identify hub genes which were involved in pathogenesis of liver injury at the protein interaction level, protein-protein interaction (PPI) data were derived from the Cytoscape

plugin Bisogenet [41], and analyzed based on the six existing PPI databases including IntAct molecular interaction database (<https://www.ebi.ac.uk/intact/>) Human Protein Reference Database (<http://www.hprd.org/>) [42–43], Molecular interaction Database (<https://mint.bio.uniroma2.it/>) [44], Database of Interacting Proteins (<https://dip.doe-mbi.ucla.edu/dip/Main.cgi>) [45], Biological General Repository for Interaction Datasets (<https://thebiogrid.org/>) [46] and Biomolecular Interaction Network Database (<http://bind.ca>) [47]. Remarkably, Bisogenet was accepted as a multi-tier application for visualization and analysis of biomolecular relationships in the field of bioinformatics due to it can integrate data from different sources in a fast and user-friendly manner, in addition, provide the suitable framework and flexible approaches to reconstruct, represent and analyze topological networks for PPI data [48].

### Network construction and analysis of components with potential liver injury

First, the components-targets (C-T) network was constructed by the interaction of the candidate compounds with the corresponding proteins that obtained from the above mentioned Cytoscape plugin Bisogenet. The topological features such as degree, betweenness, and closeness, were used to select the putative targets by means of Cytoscape plugin CytoNCA [49]. The twofold median value of node degree, the onefold median value of betweenness and closeness were applied as a cutoff point in present network. The degree of a node was defined as the number of edges connecting to a node, and the betweenness centrality was corresponded to the frequency with which shortest paths between any pair of nodes, and the closeness centrality was measured the importance of a node in a subnetwork [50]. The definitions and computational formulas of these parameters were previously defined and represented the topological importance of a node in the network. After predicting with the three parameters, the component-target interaction network was thereafter visualized with Cytoscape program (Version 3.2.1) [51]. Second, the targets-pathways (T-P) network was built through the connection of the targets and their own pathways, respectively. In addition, the pathway enrichment analysis of the candidate targets was accessible from the DAVID Bioinformatics Database (Resources 6.8, <http://david.abcc.ncifcrf.gov>), a web-based online bioinformatics resource that aimed to provide tools for the functional interpretation for large lists of genes or proteins [52]. The core pathway was screened in Omicshare 3.0 (<http://www.omicshare.com/>). Also, the pathway was annotated by employing the Reactome Pathway Database (<http://www.reactome.org>), which was an open source, expert-authored, peer-reviewed, manually curated database of reactions, pathways and biological processes [53]. Based on the C-T network and T-P network, the core target and pathway of liver injury for candidate components would be considered as the receptor protein in following molecular docking simulation.

### Molecular docking simulation

The molecular docking simulation was performed to verify the binding affinity of candidate compounds and liver injury core target [54]. First, Protein Data Bank (PDB) database (<http://www.rcsb.org/pdb/home/home.do>, updated on March 11, 2014) was used for retrieving the protein conformation of core target with liver injury, of *Homo sapiens origin* [55], meeting following criterion was recognized as appropriate protein conformation: 1) The three-dimensional protein structures were determined via X-ray crystallography; 2) The crystal resolution of protein was smaller than 3 Å; 3) The protein analysis of genotype was definite and reliable; 4) The protein conformation that had been proven and supported by published information was given the priority. Second, directly downloaded the crystal structures of the candidate targets as the file format called pdbqt from the PDB database, and the process of adding hydrogen atoms and charges, merging non-polar hydrogens bond identification and selector statics

calculations, predicting binding site and ligand deletion, superimposing homologous or mutant structures, and testing conformational changes were presented through the UCSF Chimera ([www.cgl.ucsf.edu/chimera](http://www.cgl.ucsf.edu/chimera)) [56–57] and Autodock Tool 4.0 [58–59]. Third, the rectangular boxes for the definition of binding site were predicted, the binding poses and grid box of compounds were assessed; molecular docking among candidate compounds and core target for liver injury was conducted by Autodock Vina [60–61]. Furthermore, the docking poses were ranked according to their docking scores, and the compounds with higher binding affinity were selected to illustrate their corresponding binding poses and sites via Pymol software [62]. In addition, different hydrogen-bond and hydrophobic interactions of ligand-binding sites were displayed through Ligplus software [63]. The toxic mechanism of representative compounds with higher binding affinity was explored via the following cell experiment.

### Cell culture

The normal hepatic cell (L02) cell lines were obtained from the National Infrastructure of Cell Line Resources (Chinese Academy of Medical Sciences, Beijing, China), and maintained in Dulbecco's modified Eagle's medium (DMEM, 10-013-CVR) supplemented with 10% fetal bovine serum (FBS, Hyclone), 1% penicillin and streptomycin (PS, 100 IU/ml penicillin, 100 µg/ml streptomycin, Mediatech, 30-002-CI). All cells were incubated in a humidified atmosphere at 37°C with 5% CO<sub>2</sub>.

### MTT assays

L-02 cells were trypsinized by 0.25% trypsin after reaching the confluence of 70–80% and plated in 96-well plates at the density of  $1.6 \times 10^3$  cells/plate. And L-02 cells were cultured for 24 hours in vitro before exposure to varying concentrations of different representative compounds with liver injury for further incubating in another 24 hours. Then, 20 µl of 0.25 mg/ml 3-(4,5-dimethylthiazol-2-yl)-2,5-diphenyltetrazolium bromide (MTT)-tetrazolium salts (Sigma-Aldrich Corp., St. Louis, MO, USA) in PBS was added to each hole in 96-well plates. After 4 hours of incubation, the formazan crystals were dissolved by 150 µl Dimethyl Sulphoxide (DMSO), and shocked to dissolve thoroughly, then the cell viability was measured by MTT method at 570 nm [64–65]. All experiments were repeated in triplicate independently.

### Biochemical indicators of hepatotoxicity in cell

To determine how potential liver injury-compounds affected biochemical indicators of L-02 cells, we investigated the activities of AST, ALT, LDH and ALP in cell migration capacity under the different representative compounds conditions (representative compounds group), the inhibitor conditions (inhibitor group), and the negative control. For these experiments, three replicates were made for each concentration of the different representative compounds with liver injury, and each group was established three holes and cultured in 6 times repeatedly. L02 cells were settled into 24-well plate at concentrations of  $1.6 \times 10^3$  per well for 24h and then treated with the concentrations that had been determined by MTT method of the representative candidate liver injury compounds for another 24 h. Subsequently, the supernatant extraction of L02 cells was collected and centrifuged to detect the activities of AST, ALT, LDH, and ALP by chromatometry method.

### Western blot

After the examination of biochemical indicators for hepatotoxicity in the cell, the expression of crucial liver injury protein in L02 cell lines among different groups was compared by

Western blot analysis. Briefly, the proteins from different groups were harvested and lysed using lysis buffer (Sigma-Aldrich) containing a proteinase inhibitor cocktail (Sigma-Aldrich), the equal amounts of protein were separated by electrophoresis on a pre-cast 10% SDS-polyacrylamide gel (Bio-Rad, Hercules, CA) and transferred to polyvinylidene difluoride membranes (Millipore, Bedford, MA). Next, the membrane was blocked in TBST-T containing 5% skim milk for 2 h at room temperature and probed with anti-beta-catenin, and incubated overnight with the indicated primary antibody, followed by incubation with the secondary antibodies at room temperature for another 2 h. Finally, all the immune blots were visualized by enhanced chemiluminescence (Pierce Biotechnology, Inc., Rockford, IL, USA) and western blots were performed at least three times.

### Statistical analysis

The values were presented as the mean  $\pm$  standard deviation (SD) from 3 independent experiments for 4 cell lines. The statistical analysis was performed with unpaired t-test and one-way ANOVA by GraphPad Prism 5 software (GraphPad Software, Inc, La Jolla, USA), and  $p < 0.05$  was considered to be statistically significant.

## Results

### The potential liver injury components of urate-lowering Chinese herbs

Initially, 61,236 published articles concerning drug-induced liver injury were retrieved according to above-described search strategy, a total of 171 urate-lowering Chinese herbs were collected and enrolled through the comprehensive retrieval in the present study. Additionally, 7 individual herbs exerted the obvious effects of urate-lowering, the compatibility of 134 herbs in formulas presented a synergistic combination for treating hyperuricemia, and 30 herbs against hyperuricemia can be used both alone and compatible. Through further inspection and excluded irrelevant literature, ultimately 481 articles that reported 32 candidate components from urate-lowering Chinese herbs were enrolled in present research, these components were associated with liver damage and hepatic metabolism hindrance. Remarkably, the majority of them were the simultaneously effective and toxic constituent in herbs, and the details about the component with liver injury from urate-lowering Chinese herbs were provided in [Table 1](#).

### The construction and analysis of network pharmacology

Totally, we collected 272 targets corresponding to the components with potential liver injury through the aforementioned databases, PPI networks were constructed for the putative targets that were related to 32 components with liver injury. Then, the putative C-T interaction network of liver injury consisted of 1790 nodes. Following the construction of the C-T interaction network and the calculation of three topological features (degree, betweenness, and closeness) for each core target, the screening of candidate targets was performed under the conditions of degree  $>29$ , closeness  $>0.43523$ , betweenness  $>0.00015$ , using the twofold median value of node degree, the onefold median value of betweenness and closeness in this network as a cutoff point, 153 nodes were identified as core targets including mitogen-activated protein kinase 14 (MAPK14), nitric oxide synthase and inducible (NOS2), peroxisome proliferator-activated receptor gamma (PPARG), and tumor necrosis factor (TNF). The detailed information on the core targets in the C-T interaction network was presented in [Table 2](#), the component-target interaction network and target-pathway network was illustrated in [Fig 2](#). The information of top 10 pathways was shown in [Table 3](#).

**Table 1. The details about the components with liver injury from urate-lowering Chinese herbs.**

Number	Components	Structural formula	Molecular mass
1	Arecoline	C <sub>8</sub> H <sub>13</sub> NO <sub>2</sub>	155.20
2	Saikosaponin D	C <sub>42</sub> H <sub>68</sub> O <sub>13</sub>	780.47
3	Dioscin	C <sub>45</sub> H <sub>72</sub> O <sub>16</sub>	869.06
4	Bergapten	C <sub>12</sub> H <sub>8</sub> O <sub>4</sub>	216.20
5	Xanthotoxin	C <sub>12</sub> H <sub>8</sub> O <sub>4</sub>	216.19
6	Osthole	C <sub>15</sub> H <sub>16</sub> O <sub>3</sub>	244.29
7	isopsoralen	C <sub>11</sub> H <sub>6</sub> O <sub>3</sub>	186.17
8	Tetrandrine	C <sub>38</sub> H <sub>42</sub> N <sub>2</sub> O <sub>6</sub>	622.76
9	Puerarin	C <sub>21</sub> H <sub>20</sub> O <sub>10</sub>	432.38
10	Berberine	C <sub>20</sub> H <sub>18</sub> ClNO <sub>4</sub>	371.82
11	Baicalin	C <sub>21</sub> H <sub>18</sub> O <sub>11</sub>	446.36
12	Baicalein	C <sub>15</sub> H <sub>10</sub> O <sub>5</sub>	270.24
13	Curcumin	C <sub>21</sub> H <sub>20</sub> O <sub>6</sub>	368.38
14	Sophocarpine	C <sub>15</sub> H <sub>22</sub> N <sub>2</sub> O	246.35
15	Sophoraflavanone G	C <sub>25</sub> H <sub>28</sub> O <sub>6</sub>	424.49
16	Matrine	C <sub>15</sub> H <sub>24</sub> N <sub>2</sub> O	248.37
17	Kurarinone	C <sub>26</sub> H <sub>30</sub> O <sub>6</sub>	438.52
18	Oxysophocarpine	C <sub>15</sub> H <sub>22</sub> N <sub>2</sub> O <sub>2</sub>	262.35
19	Oxymatrine	C <sub>15</sub> H <sub>24</sub> N <sub>2</sub> O <sub>2</sub>	264.37
20	Gentiopicroside	C <sub>16</sub> H <sub>20</sub> O <sub>9</sub>	356.33
21	Reynosion	C <sub>15</sub> H <sub>20</sub> O <sub>3</sub>	248.32
22	Santamarine	C <sub>15</sub> H <sub>20</sub> O <sub>3</sub>	248.32
23	Aucklandiae	C <sub>15</sub> H <sub>24</sub> O	220.00
24	Elemol	C <sub>15</sub> H <sub>26</sub> O	222.37
25	Dehydrocostuslactone	C <sub>15</sub> H <sub>18</sub> O <sub>2</sub>	230.31
26	Artesunate	C <sub>19</sub> H <sub>28</sub> O <sub>8</sub>	384.42
27	Colchicine	C <sub>22</sub> H <sub>25</sub> NO <sub>6</sub>	399.44
28	Rutaecarpine	C <sub>18</sub> H <sub>13</sub> N <sub>3</sub> O	287.32
29	Evodiamine	C <sub>19</sub> H <sub>17</sub> N <sub>3</sub> O	303.37
30	1-Tetrahydropalmatine	C <sub>21</sub> H <sub>25</sub> NO <sub>4</sub>	355.43
31	Genipin	C <sub>11</sub> H <sub>14</sub> O <sub>5</sub>	226.23
32	Geniposide	C <sub>17</sub> H <sub>24</sub> O <sub>10</sub>	388.37

<https://doi.org/10.1371/journal.pone.0216948.t001>

As shown in Fig 3, the biological processes by the MAPK signal pathway were often associated with the higher target hit quantity. Especially, the MAPK signal pathway had been indicated to contribute to liver metabolic changes, liver steatosis, and hepatic cell apoptosis during the progression of gluconeogenesis and lipid metabolism. As the major p38 MAPK isoform, p38α ubiquitously expressed at high levels in most cell types and played a pivotal role in elevating liver enzymes, survival genes, DNA damage, oxidative stress, inflammation response due

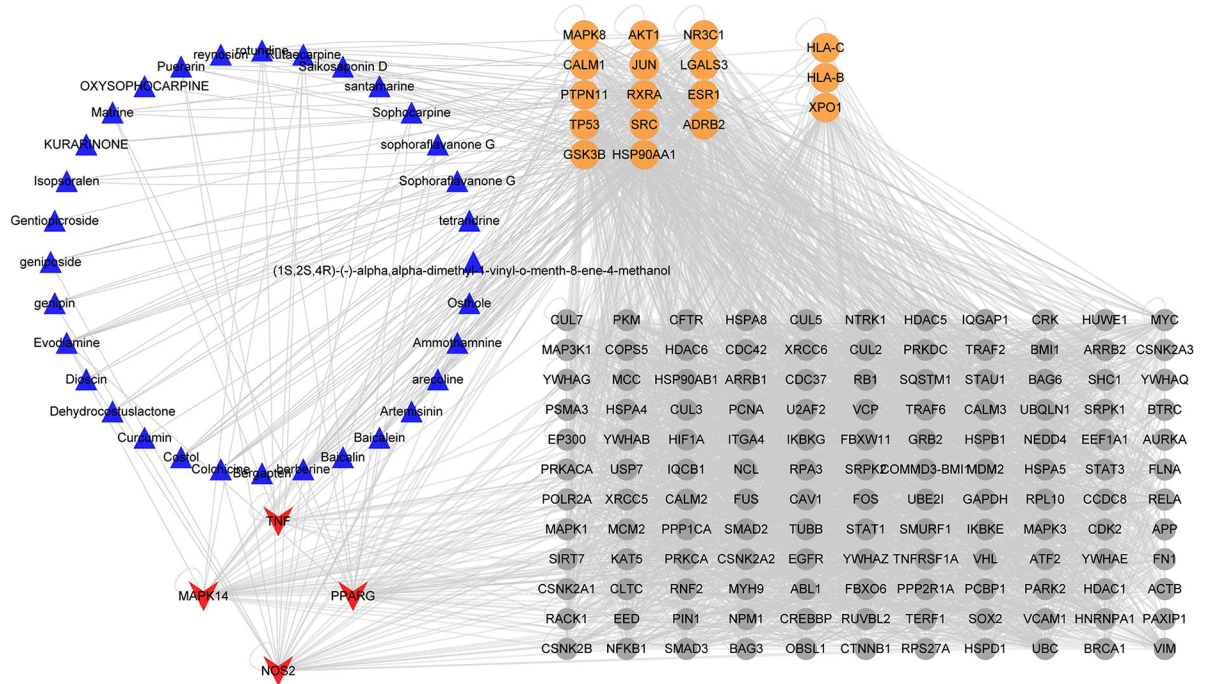
**Table 2. The detail about core target in the component-target interaction network.**

Target	Degree	Betweenness	Closeness
MAPK14	237	0.028579	0.506369
NOS2	157	0.006274	0.470542
PPARG	155	0.01105	0.499024
TNF	116	0.019764	0.44151

<https://doi.org/10.1371/journal.pone.0216948.t002>



A



B

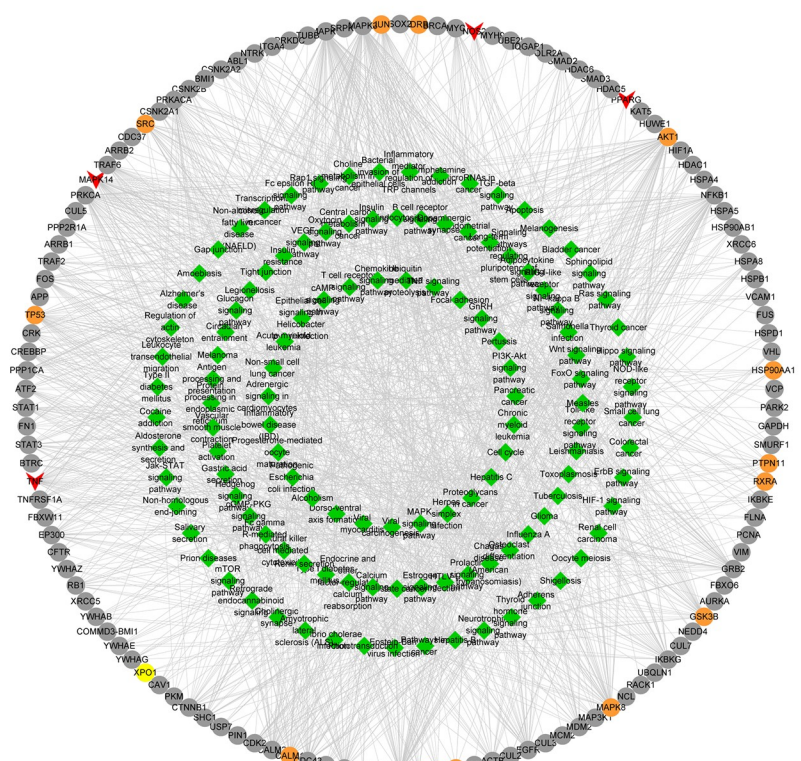


**Fig 2. Component-target interaction network and target-pathway network.** Note: (A). The potential liver injury components urate-lowering Chinese medicine are indicated by blue triangles, the core targets are indicated by red arrows; the direct targets of components and “liver injury” are represented by yellow circles, and the interaction targets of components and “liver injury” are gray. (B). The pathways are represented by green diamond. The targets are indicated by red arrow; the direct target of the compound and disease” are represented by yellow circle, and the interacting proteins are represented by gray circle. To get an initial sense of the biological processes and pathways enriched by putative targets that were relative with liver injury, the functional enrichment analysis was conducted based on DAVID. And the results were classified into several signaling pathways, including pathways in cancer,

Epstein-Barr virus infection, Viral carcinogenesis, p38 $\alpha$  mitogen-activated protein kinase (MAPK) signaling pathway, the immune system, signal transduction, gene expression, cell cycle, DNA replication, and other processes in Fig 2.

<https://doi.org/10.1371/journal.pone.0216948.g002>

to negatively regulate the G1/S and G2/M cell cycle transitions [66–68]. Accordingly, p38 $\alpha$  was chosen as the core target for further elucidating the related mechanisms of liver injury in following molecular docking simulation.

### Molecular docking simulation

In present work, molecular docking was carried out between all of the 32 candidate compounds with liver injury and p38 $\alpha$ . To validate the docking method and docking accuracy, the different compounds was docked into the binding site of p38 $\alpha$ , respectively. Both the ligand and receptor were isolated from the complex crystal structure in the PDB database. The results indicated that there were 6 representative compounds with an acceptable reliability of the docking method (binding free energy  $\leq -8$  kcal/mol) for the p38 $\alpha$ , and these compounds included diosgenin, baicalin, saikosaponin D, tetrandrine, rutaecarpine, and evodiamine, besides, the structures of these 6 representative compounds with strong binding capacity for p38 $\alpha$  were depicted in Fig 4, the information of binding free energy for 32 potential liver injury components was shown in Table 4. Moreover, the main binding mode between the pairs of p38 $\alpha$  and compounds was hydrogen bonding based on the analysis of Pymol and Ligplot, the 6 representative compounds with strong binding capacity were taken as the examples, the docking results between these compounds and p38 $\alpha$  were shown in Fig 5. The molecular docking results laid the material foundation for the observation of biological effects subsequently.

### Evaluation of hepatotoxicity for representative components with liver injury

The hepatotoxicity for representative components from urate-lowering Chinese herbs was evaluated by investigating on L-02 by means of incubating with various concentrations of different components. The results of MTT assay demonstrated that diosgenin, rutaecarpine and evodiamine could achieve the good potency inhibitor against the cell viability of L-02 at a dose of 5  $\mu$ mol/L. Tetrandrine and saikosaponin D were associated with the lower cell survival rate at the dose of 60–90  $\mu$ mol/L. These results of biochemical analyses were consistent with the findings of previous network pharmacology. Interestingly, baicalin had the trend of proliferative effects on L-02 at the dose of 2000  $\mu$ mol/L, indicating this compound may not cause liver

**Table 3. The detail of the top 10 pathways in the target-pathway interactive network.**

Pathway	Target hit quantity	P-value
Pathways in cancer	42	4.33E-20
Epstein-Barr virus infection	39	4.55E-29
Viral carcinogenesis	31	8.26E-19
MAPK signaling pathway	30	3.88E-15
Hepatitis B	28	9.02E-20
PI3K-Akt signaling pathway	28	2.96E-10
Herpes simplex infection	26	5.44E-15
HTLV-I infection	26	1.26E-11
Proteoglycans in cancer	25	3.83E-13
Neurotrophin signaling pathway	23	4.44E-16

<https://doi.org/10.1371/journal.pone.0216948.t003>

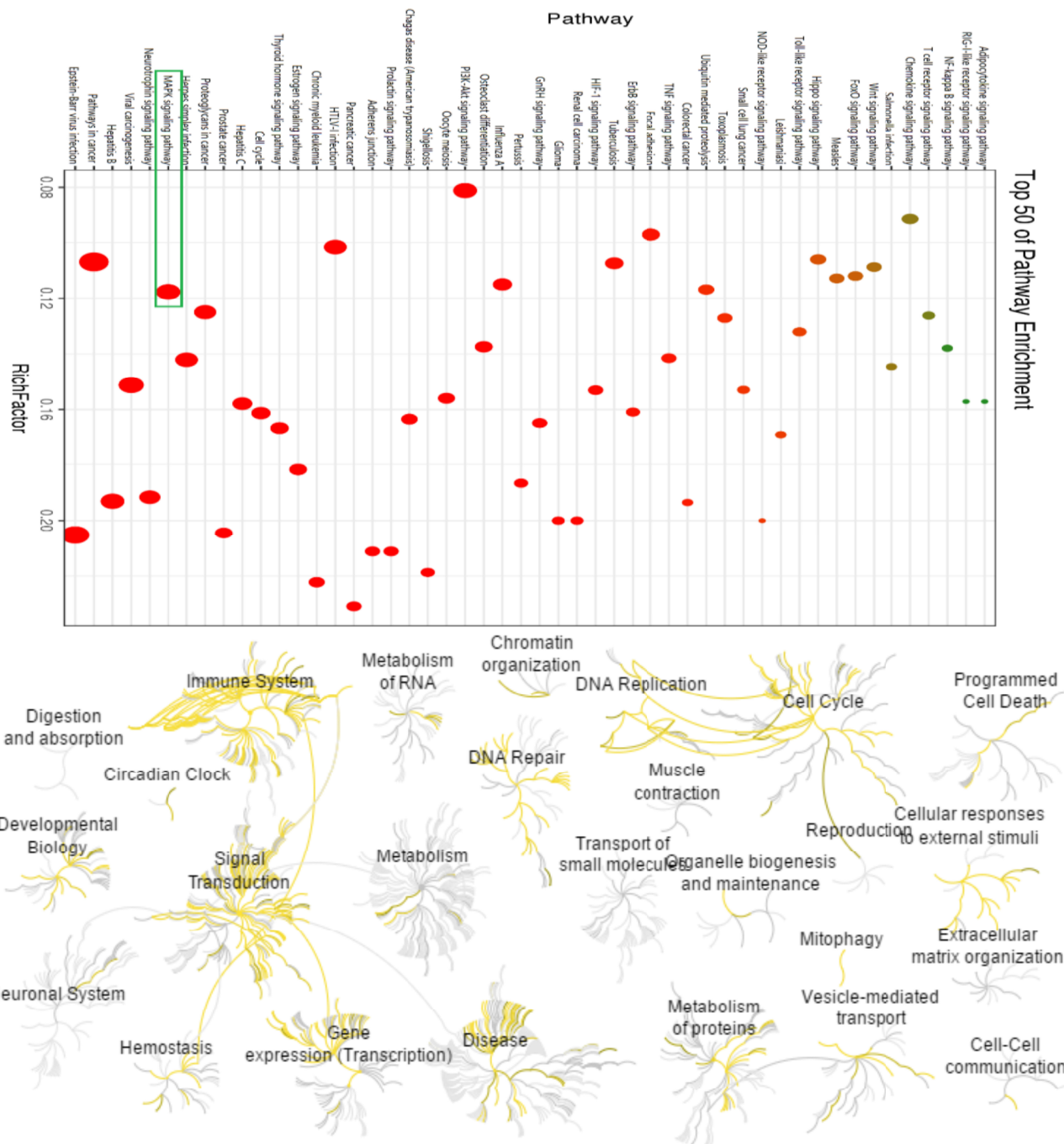


**Fig 3. Distribution and the bubble map of core pathways.** Note: (A.) The vertical axis is the path name and the horizontal axis is the Rich Factor value. The larger the P-value, the higher the channel enrichment; the size of the point indicates the number of enriched targets; the color of the dots is red to green. The value is from small to large. (B.) The yellow to brown pathway lines represent the pathways for important target enrichment, from yellow to brown indicating that the pathway P-values are small to large.

<https://doi.org/10.1371/journal.pone.0216948.g003>

cell injury compared to others. In accordance with the results of cells, the order of hepatotoxicity by potential liver injury components may be diosgenin, rutaecarpine, evodiamine, tetrandrine, saikosaponin D and baicalin. The specific composition information was shown in S1

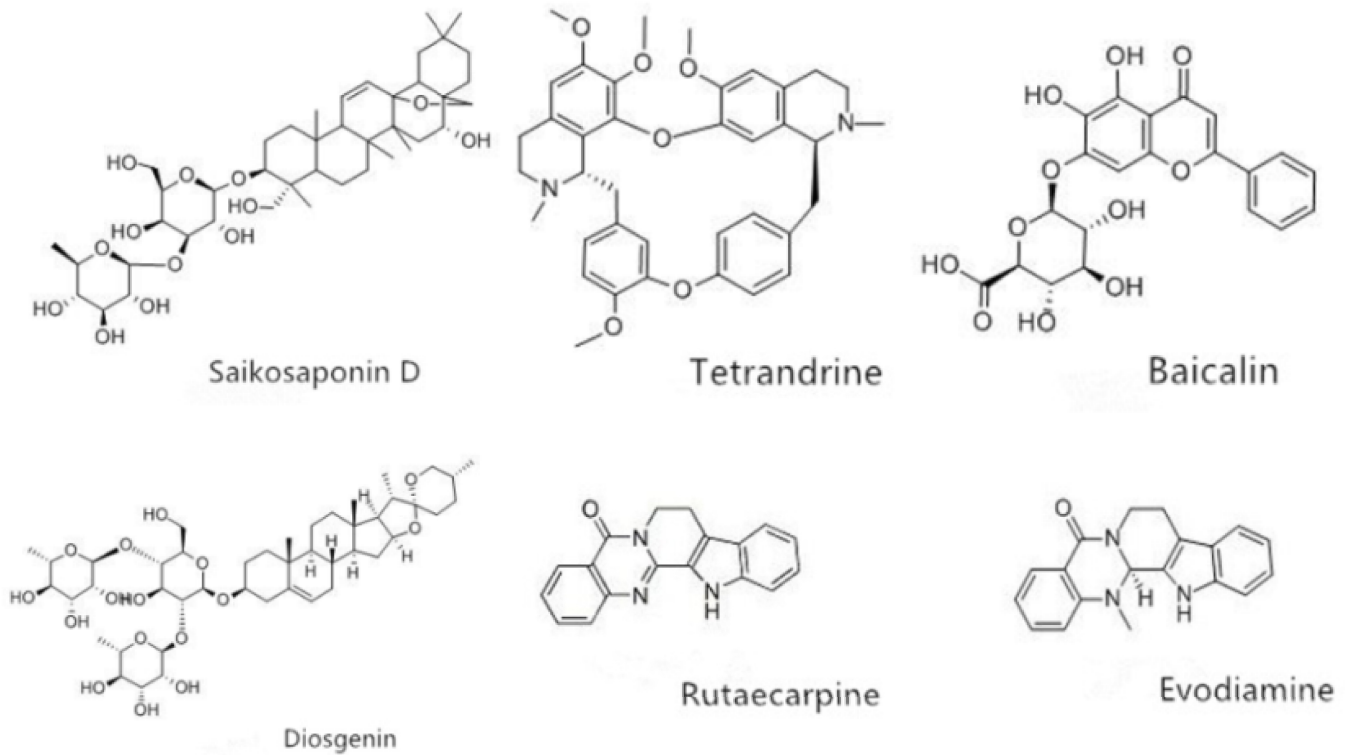


**Fig 4. The structure of 6 compounds with strong binding capacity for p38.**

<https://doi.org/10.1371/journal.pone.0216948.g004>

**Table.** In each of the drug-administered groups, three concentrations before and after the cell viability significantly decreased were subjected to subsequent experiments.

The results of the colorimetric assay for investigating ALT, AST, LDH, and ALP activities among different components groups, revealed that the levels of ALT, AST, LDH and ALP

**Table 4. Binding free energy for 32 components with potential liver injury.**

Number	Components	Binding free energy (kcal/mol)	Number	Components	Binding free energy (kcal/mol)
1	Diosgenin	-8.9	17	Santamarine	-6.8
2	Baicalin	-8.3	18	1-Tetrahydropalmatine	-6.8
3	Saikosaponin D	-8.2	19	Gentiopicroside	-6.7
4	Tetrandrine	-8.2	20	Dehydrocostuslactone	-6.7
5	Rutaecarpine	-8.2	21	Reynosion	-6.7
6	Evodiamine	-8	22	Sophocarpine	-6.6
7	Kurarinone	-7.9	23	Xanthotoxin	-6.6
8	Sophoraflavanone G	-7.6	24	Aucklandiae	-6.5
9	Artemisinin	-7.3	25	Matrine	-6.5
10	Puerarin	-7.2	26	Ammothamine	-6.5
11	Baicalein	-7.2	27	isopsoralen	-6.4
12	Berberine	-7.1	28	Osthole	-6.1
13	Curcumin	-7	29	Bergapten	-5.9
14	Genipin	-6.9	30	Geniposide	-5.4
15	Colchicine	-6.9	31	Elemol	-5.3
16	Oxysophocarpine	-6.9	32	Arecoline hydrobromide	-4.2

<https://doi.org/10.1371/journal.pone.0216948.t004>

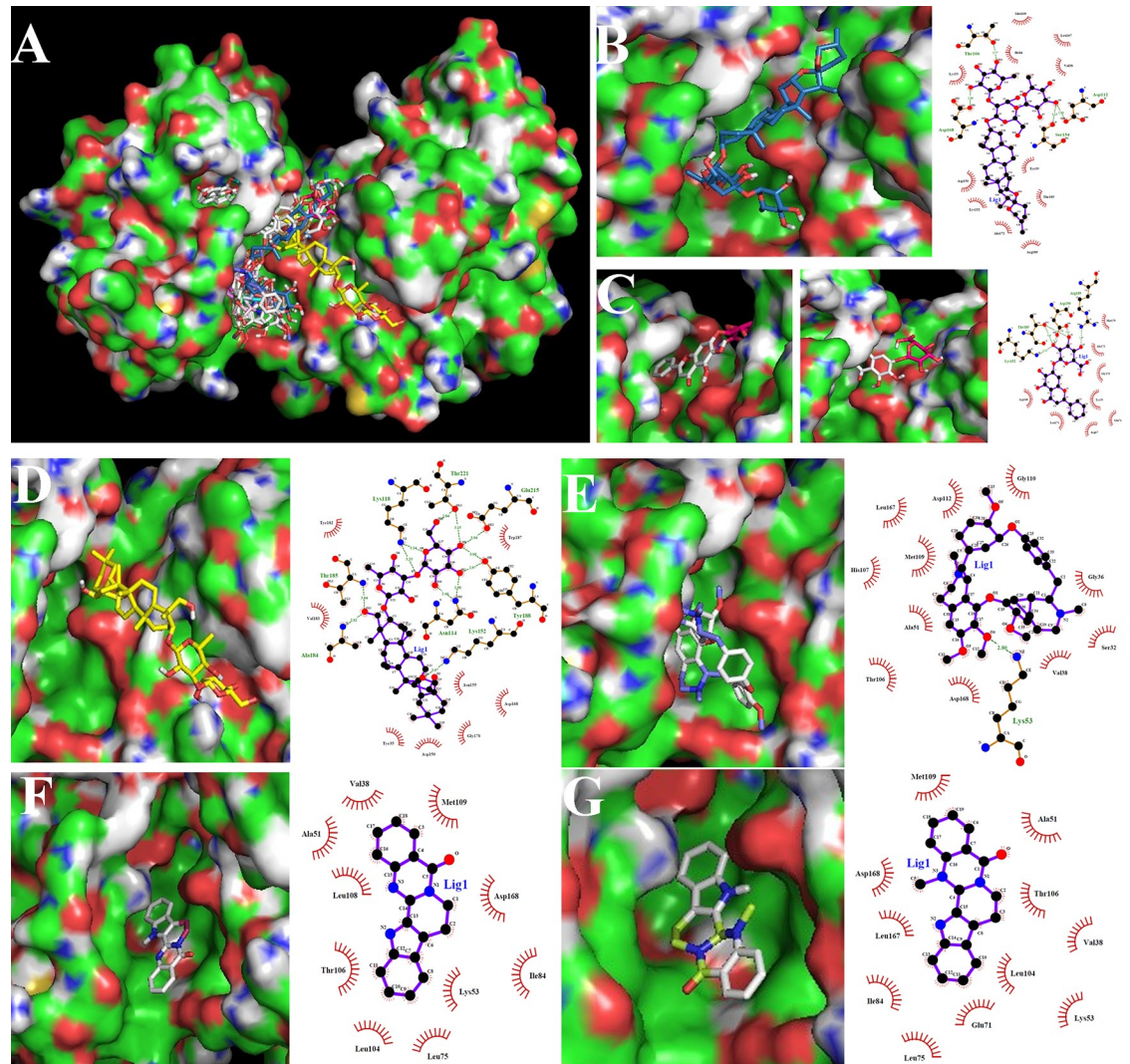


**Fig 5. Docking modes between potential liver damage components and p38.** Note: (A.) 32 potential liver injury components have entered the p38 $\alpha$  protein active pocket. (B.) The small molecule of diosgenin penetrated into the active pocket, and mainly forms four hydrogen bonds with the Thr106, Asp168, Asp112 and Ser154 residues on the protein, atotal of 15 residues were bound by hydrophobic interaction on the p38 $\alpha$ . (C.) The baicalin small molecule completely penetrated into the active pocket, forming 11 hydrogen bonds with the Arg189, Thr185, Asp150, Lys152, Tyr35 residues on the protein, and the sugar moiety contributed 9 hydrogens. The aglycone part contributed 2 hydrogen bonds, and more hydrophobic interaction with the protein. The hydrophobic interaction residues of the baicalin molecule were 13. (D.) The saikosaponin D molecule completely entered the active pocket, mainly with Glu215 and Thr221 on the protein, Tyr188, Asn114, Lys118, Ala184, Thr185, Lys152 residues form 13 hydrogen bonds, a total of 16 hydrophobic residues. (E.) Tetrandrine small molecules deeped into the active pocket, forming a hydrogen bond with Lys53, and 13 residues formed a hydrophobic effect. (F.) Rutaecarpine completely entered the active pocket and formed a hydrophobic interaction with 10 residues. (G.)Evodiamine completely entered the active pocket, and 11 residues formed a hydrophobic effect.

<https://doi.org/10.1371/journal.pone.0216948.g005>

increased obviously in potential liver injury components groups, suggesting that these components could exert hepatotoxicity in L-02 cells. In regard to baicalin, the baicalin group 1000 $\mu$ mol/L were associated with higher levels of ALT, AST, LDH and ALP than the blank group and the difference between both groups was not statistically significant, while the dose of 2000 $\mu$ mol/L could significantly increase the levels of ALT, AST, LDH and ALP than the blank group. Thereby baicalin could inhibit the proliferation of L-02 cells instead of inducing the cell damage. The specific composition information was shown in Table 5.

**Table 5. ALT, AST, LDH, ALP enzyme activity of L-02 cells interfered with the representative components with liver injury from urate-lowering Chinese herbs.**

Group		ALT(U/L)	AST(U/L)	LDH(U/L)	ALP (King's unit /100ml)
Dioscin	Blank	5.81±0.23	360.61±16.38	1.79±0.25	16.72±0.90
	Control	7.28±1.21	533.67±35.52**	1.84±0.09	17.30±1.02
	1µmol/L	7.53±0.61**	523.02±30.77**	1.58±0.39	16.03±1.60
	5µmol/L	6.88±0.50**	524.30±19.64**	3.67±0.30** <sup>ΔΔ</sup>	15.58±1.17
	10µmol/L	7.53±0.11**	561.38±74.95**	4.58±0.64** <sup>ΔΔ</sup>	15.91±0.48
Baicalin	Blank	1.52±0.80	502.37±50.60	1.03±0.24	1.55±0.19
	1000µmol/L	4.45±1.09*	690.76±33.24**	0.81±0.10	2.03±0.44
	2000µmol/L	4.48±0.13**	824.64±39.22**	0.84±0.18**	1.94±0.21*
Saikosaponin D	Blank	8.00±2.94	382.43±40.86	1.32±0.05	15.78±1.68
	Control	7.74±1.64	611.11±60.86**	1.13±0.12*	15.83±0.82
	50µmol/L	7.75±1.25	560.72±37.00**	1.13±0.25	15.58±1.07
	70µmol/L	14.41±0.60** <sup>ΔΔ</sup>	1472.87±52.32** <sup>ΔΔ</sup>	0.95±0.17**	23.12±2.09** <sup>ΔΔ</sup>
	90µmol/L	16.00±0.74** <sup>ΔΔ</sup>	1497.42±60.20** <sup>ΔΔ</sup>	1.00±0.08**	22.19±1.23** <sup>ΔΔ</sup>
Tetrandrine	Blank	3.43±0.21	589.59±69.45	0.92±0.10	14.36±0.82
	Control	4.52±0.80*	577.48±56.62	0.98±0.20	15.00±0.60
	40µmol/L	4.36±0.35*	713.48±49.44* <sup>Δ</sup>	0.79±0.08	16.55±0.71* <sup>Δ</sup>
	60µmol/L	5.01±1.20*	705.81±98.97 <sup>Δ</sup>	0.82±0.16	16.39±0.81*
	80µmol/L	4.84±0.86*	736.08±77.41* <sup>Δ</sup>	0.93±0.07	17.45±0.35** <sup>ΔΔ</sup>
Rutaecarpine	Blank	2.66±0.99	588.31±96.50	1.08±0.14	2.25±0.48
	Control	9.42±1.62**	1072.79±58.59**	1.76±0.50*	5.86±0.09**
	5µmol/L	9.90±0.99**	1075.18±91.40**	1.62±0.04**	5.77±0.54**
	10µmol/L	8.81±1.85**	1127.68±56.72**	1.54±0.36*	5.67±0.12**
	15µmol/L	9.33±1.85**	1000.00±61.27**	1.71±0.16**	5.54±0.57**
Evodiamine	Blank	6.04±0.54	466.02±72.08	1.00±0.09	15.00±0.46
	Control	6.67±1.32	614.08±52.56*	0.56±0.19**	14.77±1.15
	5µmol/L	7.07±0.38*	658.98±40.96**	0.50±0.16**	15.54±0.25
	6µmol/L	6.74±0.73	597.09±44.76*	0.57±0.17**	16.42±0.66*
	7µmol/L	6.22±1.15	612.86±52.77*	0.49±0.23**	16.42±0.87*

\*P<0.05

\*\*P<0.01 compared with the blank group. <sup>Δ</sup>P<0.05, <sup>ΔΔ</sup>P<0.01 compared with the control group, n = 4.

<https://doi.org/10.1371/journal.pone.0216948.t005>

### The results of Western blot assay

According to the results of network pharmacology, we examined the expression levels of p38α. Antibodies was used as follows: p38α antibody (CST, 9218S), Phospho-p38 MAPK (Thr180/ Tyr182) (D3F9) XP Rabbit mAb (CST, 4511S), IgG H&L (HRP) (Abcam, ab6721). As shown in Fig 6, the results of western blot indicated that the ratios of p-p38α/p38α expression were all increased in L-02 cells treated by 10µmol/L diosgein, 2000µmol/L baicalin, 60µmol/L terandrine and 6µmol/L evodiamine compared with the blank groups. While each dose in saikosaponin D group showed relatively weak signal intensities in the expression of p-p38α/p38α. The Specific specific composition information is was shown in S3 Table. Overall, the mechanism of liver injury influenced by diosgein, baicalin, terandrine and evodiamine in correlation with the western blot data was related to the increased expression of p38α. However, the mechanism of saikosaponin D causing liver injury still remained unclear.

To further and fully elucidating the mechanism of the liver injury caused by the representative compounds from urate-lowering Chinese herbs, we chose the p38α inhibitor, SB203580 to verify our findings. Seemingly, the ALT, AST, ALP, and LDH activities of each group

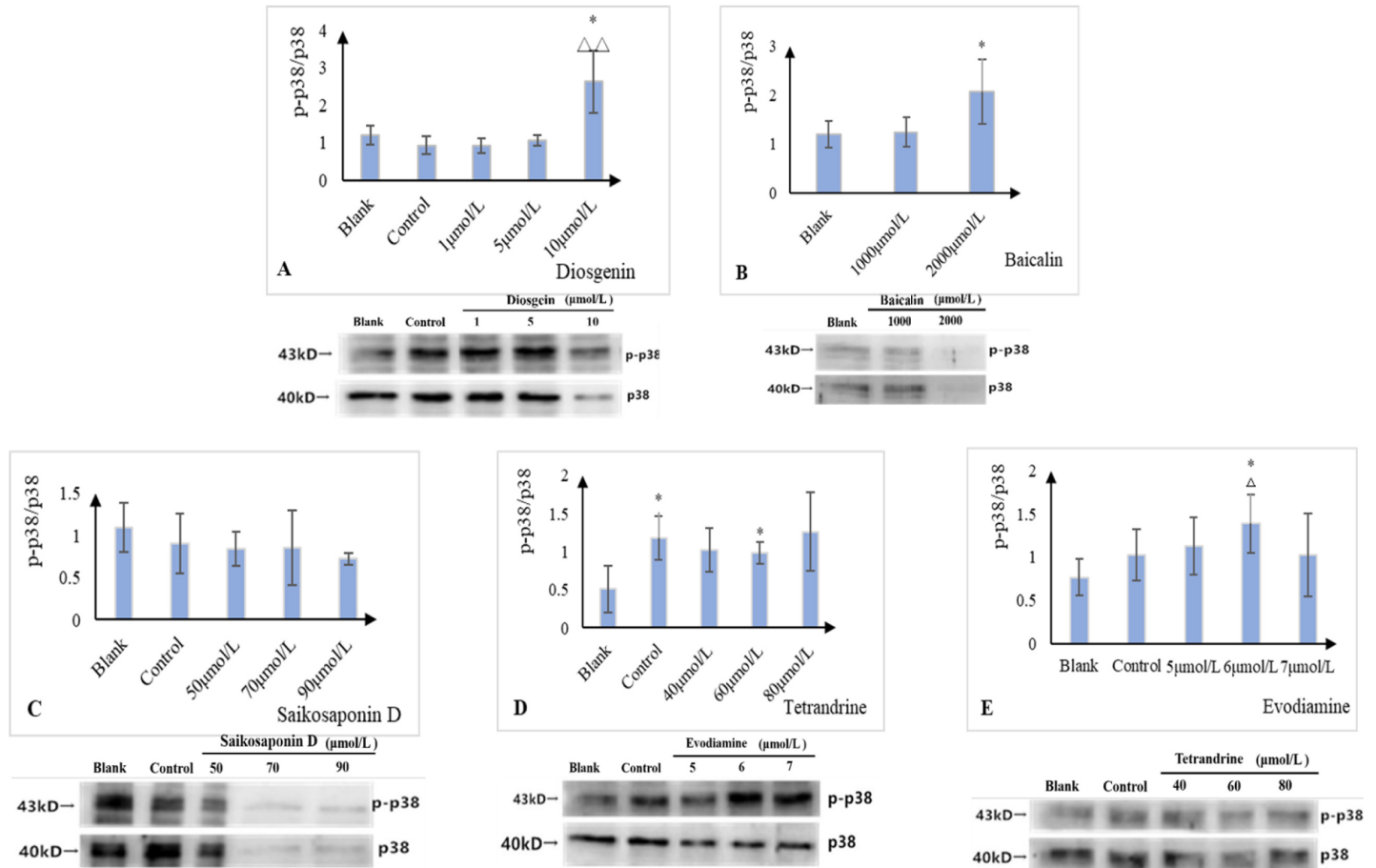


**Fig 6. Effect of potential liver injury components on the expression of p38 protein.**

<https://doi.org/10.1371/journal.pone.0216948.g006>

decreased to varying degrees under the influence of inhibitor. The specific composition information was shown in [S2 Table](#). Also, the result indicated that SB203580 could attenuate the component-induced cell damage of L-02 cells. Similarly, as shown in [Fig 7](#), the ratios of p-p38 $\alpha$ /p38 $\alpha$  expression were all decreased in L-02 cells treated by the combination of components and SB203580 compared with the blank groups. Combined with changes in enzymatic indicators, it is suggested that the mechanism of the liver injury caused by the representative compounds from urate-lowering Chinese herbs may be implicated into the activation of p38 $\alpha$ , by contrast, SB203580 may ameliorate L-02 cell injury induced by the representative components. The Specific specific composition information is was shown in [S4 Table](#).

## Discussion

Current study, the approaches of the literature mining, network pharmacology, molecular docking, and cell experiment validation were undertaken to decipher the underlying drug-induced liver injury molecular mechanisms of urate-lowering Chinese herbs. Our study revealed that the representative compounds with liver injury from urate-lowering Chinese herbs included diosgenin, rutaecarpine, evodiamine, tetrandrine, saikosaponin D and baicalin, moreover, MAPK signaling pathway (p38) was the main action pathways closely related to liver injury for these compounds, and the mechanism of the liver injury induced by these compounds may be associated with promoting the expression of p38 $\alpha$ .

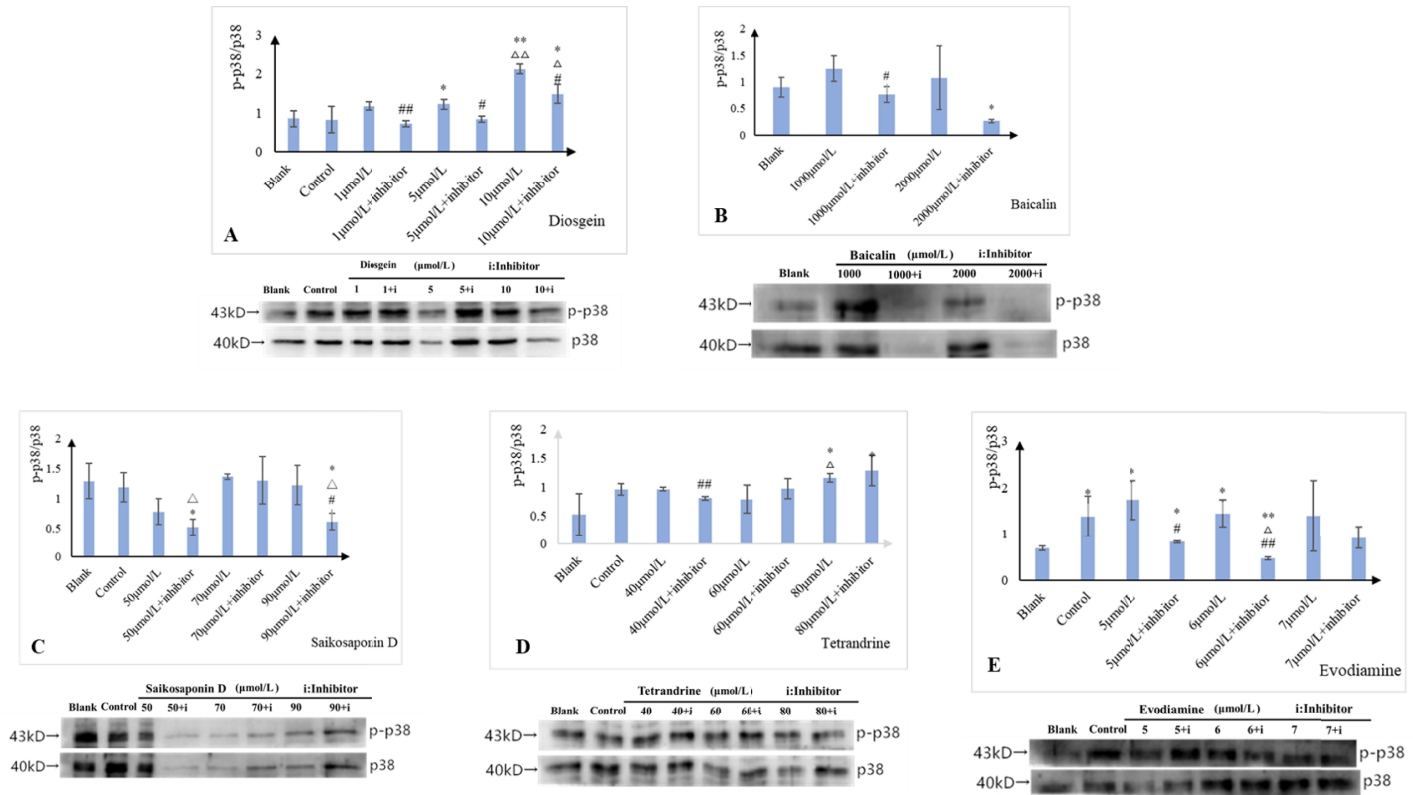


Fig 7. Effects of potential liver injury components on L-02 cells p38 protein expression activity with inhibitor.

<https://doi.org/10.1371/journal.pone.0216948.g007>

Through the comprehensive searching of published experiment and literature data, we identified 171 Chinese herbs and TCM formulations that were beneficial for treating hyperuricemia, these Chinese herbs covered the categories of dampness-eliminating, blood-activating and stasis-removing, deficiency-supplementing and so on. Also, the nature of these herbs' distribution was widespread, and they produced satisfactory therapeutic effects for different syndrome types of hyperuricemia clinically; however, there were ADR reports of liver injury for some urate-lowering Chinese herbs during long-term treatment of hyperuricemia. According to the pharmacological studies, as the a bisbenzylisoquinoline alkaloid isolated from the Chinese herb *Stephania tetrandra* S. Moore., trandrine-induced mitochondrial dysfunction and the sources of oxidative stress may contribute to the apoptosis of live cells, and the overexpression of CYP2E1 could enhance the tetrandrine-induced cytotoxicity [69–70]. In addition, the aqueous extract of *Evodiae fructus* could trigger the liver cell death signaling, and the hepatotoxicity mechanisms were related to the dehydrogenation of evodiamine and rutaecarpine that may cause toxicities through the formation of electrophilic intermediates via CYP3A4 inactivation [71–72]. To address the liver injury mechanisms of compounds from urate-lowering Chinese herbs, we collected and analyzed the research in the field of drug-induced liver injury, a total of 32 candidate compounds were obtained through. Several of the potential liver injury targets of active compounds from urate-lowering Chinese herbs were identified by means of network pharmacology, among them, the MAPK protein yielded the core target with the higher degree centrality in our research. Recent medical studies confirm that it plays the crucial roles in diverse developmental and physiological processes involving in the cell response to outside stimuli by activating and regulating the client protein, for example, it also has been



proven that p38 is closely connected with the stress, physical and chemical reactions within the cells [73–75]. As the ubiquitously expressed prototype member of the MAPK family, the expression of p38 $\alpha$  is abundant in most tissues in response to various extracellular stimuli in different organisms [76–77], p38 $\alpha$  pathway is an essential protein of proliferation, differentiation, migration, survival, apoptosis, and autophagy of cells, the response to actin remodeling, angiogenesis and DNA damage has been highlighted over the last decade, hence, the p38 $\alpha$  was selected as the protein receptor that might be associated with liver injury for molecular docking [78–79]. With regard to the normal liver cell, the p38 activation might connect with triptolide-induced hepatotoxicity in rats, and play an important role both in the hepatic expression of proinflammatory cytokines and development of inflammation-related liver damage [80–81]. In summary, the p38 protein possesses an interesting area of research in liver injury. Furthermore, according to the docking scores between 32 candidate compounds and p38, a total of 6 representative compounds (diosgenin, rutaecarpine, evodiamine, tetrandrine, saikosaponin D and baicalin) with a high affinity were selected to cell experiments validation subsequently.

We performed the cell experiment in L-02 cells to confirm and highlight the liver injury mechanism of 6 representative compounds, due to the L-02 cells are widely applied to investigate the underlying mechanism of hepatoprotective effects or cytotoxicity recently [82–83]. Remarkably, the experimental works and clinical reports have revealed that ALT, AST, LDH, ALP activity are increased in the condition of liver damage, among the liver injury markers, ALT and AST are probably the most commonly used in both clinical diagnosis and research involving liver damage for several decades [84–85]. After the investigation the activities of AST, ALT, LDH, and ALP under 6 representative compounds, the results revealed that these compounds could lead to a significant increase of AST, ALT, LDH, and ALP to cause L-02 cell damage. Besides, baicalin could inhibit the proliferation of L-02 cells instead of inducing the cell damage because it did not achieve the significant increase of AST, ALT, LDH and ALP the dose of 2000 $\mu$ mol/L. Furthermore, the results of western blot demonstrated that the mechanism of liver injury induced by diosgenin, evodiamine, tetrandrine, and baicalin was correlated with increase the expression of p-p38 $\alpha$ /p38 $\alpha$ . However, the expression of p-p38 $\alpha$ /p38 $\alpha$  under the varying dose of saikosaponin D was without significant change. It has been validated that Saikosaponin D may block PDGF-BB and TGF- $\beta$ 1-induced cell proliferation and migration, inhibit proliferation and activation of HSC-T6 via decreasing phosphorylation of p38 [86]. Taken together, Saikosaponin D mainly played an indirect role in the regulation of p38 expression through activating other pathways, this point reflects the complexity of pharmaceutical distribution and metabolize in vivo. Herein, it is hard to extract the protein in rutaecarpine group owing to the massive cell death caused by the cytotoxicity of rutaecarpine and solubilizers. Based on the experimental works and clinical reports, SB203580 was accepted as the pyridinyl imidazole inhibitor of p38 with its favorable selectivity, which controls the various inflammatory responses and cellular stresses [87–88]. Interestingly, according to modern pharmacological research, the local application of p38 agonist anisomycin increased new bone formation in distraction osteogenesis, whereas SB203580 has the promising activity to decrease it through inhibiting p38 [89]. And it is demonstrated that the novel mechanism of SB203580 is relative to activate directly AhR-induced Cyp1a1 gene expression in an AhR-dependent manner [90]. In this regard, the SB203580 at the dose of 20 $\mu$ mol/L was supplemented in cell culture to observe the levels of AST, ALT, LDH and ALP, and the expression of p-p38 $\alpha$ /p38 $\alpha$ ; the relative results displayed that the liver injury mechanism of representative compounds with potential hepatotoxicity was closely related to p38 activation, SB203580 modulates the downstream signals to p38 and reduces drug-induced liver injury. Nevertheless, SB203580 could not reverse the process of cell damage induced by compounds with hepatotoxicity, it

suggested that the cell damage was involved and cooperated with other pathways. Although the further animal studies in vivo and pharma-toxicology studies will be pivotal for supporting our findings, the results of present study provide an overview of the liver injury mechanism induced by Chinese herbs from the network perspective and bioinformatics approach, the research route, research method, and finding can be valuable and beneficial for the identification and development of compounds with hypotoxicity from Chinese herbs.

## Conclusions

Overall, based on the bioinformatics approaches to combine the network pharmacology, computer simulation and molecular biology experiments, our results demonstrated that the compounds with potential liver injury from urate-lowering Chinese herbs, diosgenin, rutaecarpine, evodiamine, tetrandrine, saikosaponin D and baicalin, could lead to the decline the survival rate of L-02 cell, increase the activities of AST, ALT, LDH and ALP cell-culture medium, enhance the expression of p-p38/p38, and the p38 inhibitor could achieve the trend of regulating and controlling liver injury. These research findings bring further support to the growing evidence that the mechanism of the liver injury induced by the compounds from urate-lowering Chinese herbs may be associated with the activation of p38 $\alpha$ .

## Supporting information

**S1 Table. Effects of potential liver injury components on L-02 cells viability.** \*P<0.05, \*\*P<0.01 compared with the control group, n = 6.

(PDF)

**S2 Table. ALT, AST, LDH, ALP enzyme activity of L-02 cells interfered with the potential liver injury components and inhibitor.** \*P<0.05, \*\*P<0.01 compared with the blank group.  $\Delta$ P<0.05,  $\Delta\Delta$ P<0.01 compared with the control group, n = 4.

(PDF)

**S3 Table. Expression of p-p38 $\alpha$ /p38 $\alpha$  in L-02 cells interfered with the potential liver injury components.** \*P<0.05, \*\*P<0.01 compared with the blank group. Extract protein after 24 hours of incubation. Compared with the control group,  $\Delta$ P<0.05,  $\Delta\Delta$ P<0.01, n = 4.

(PDF)

**S4 Table. Expression of p-p38 $\alpha$ /p38 $\alpha$  in L-02 cells interfered with the potential liver injury components and inhibitor.** \*P<0.05, \*\*P<0.01 compared with the blank group. Extract protein after 24 hours of incubation. Compared with the control group,  $\Delta$ P<0.05,  $\Delta\Delta$ P<0.01, n = 4.

(PDF)

## Acknowledgments

The authors are very appreciative of the entire participants for their support and help in the paper editing and publishing.

## Author Contributions

**Conceptualization:** Fan Li, Zhi-Jian Lin, Bing Zhang.

**Data curation:** Fan Li, Yi-Zhu Dong, Dan Zhang, Xiao-Meng Zhang.

**Formal analysis:** Fan Li, Yi-Zhu Dong.

**Methodology:** Fan Li, Dan Zhang, Xiao-Meng Zhang, Zhi-Jian Lin.

**Supervision:** Bing Zhang.

**Validation:** Fan Li.

**Visualization:** Fan Li, Yi-Zhu Dong.

**Writing – original draft:** Fan Li, Yi-Zhu Dong, Dan Zhang.

**Writing – review & editing:** Yi-Zhu Dong, Dan Zhang, Xiao-Meng Zhang, Zhi-Jian Lin, Bing Zhang.

## References

1. Becker MA, Schumacher HR Jr, Wortmann RL, MacDonald PA, Eustace D, Palo WA, et al. Febuxostat compared with allopurinol in patients with hyperuricemia and gout. *New England Journal of Medicine*. 2006; 353(23): 2450–2461. <https://doi.org/10.1056/NEJMoa050373> PMID: 16339094
2. Merriman TR. An update on the genetic architecture of hyperuricemia and gout. *Arthritis Research & Therapy*. 2015; 17(1): 98. <https://doi.org/10.1186/s13075-015-0609-2> PMID: 25889045
3. Maharani N, Kuwabara M, Hisatome I. Hyperuricemia and Atrial Fibrillation: Possible Underlying Mechanisms. *International Heart Journal*. 2016; 57(4). <https://doi.org/10.1536/ihj.16-192> PMID: 27396561
4. Jin C, Chunxia W, Guang Z, Xiang J, Yanxun L, Xiubin S, et al. Incidence and simple prediction model of hyperuricemia for urban han chinese adults: a prospective cohort study. *International Journal of Environmental Research & Public Health*. 2017; 14(1):67. <https://doi.org/10.3390/ijerph14010067> PMID: 28085072
5. Li C, Hsieh MC, Chang SJ. Metabolic syndrome, diabetes, and hyperuricemia. *Current Opinion in Rheumatology*. 2013; 25(2): 210–216. <https://doi.org/10.1097/BOR.0b013e32835d951e> PMID: 23370374
6. Qiu L, Cheng XQ, Wu J, Liu JT, Xu T, Ding HT, et al. Prevalence of hyperuricemia and its related risk factors in healthy; adults from northern and northeastern Chinese provinces. *Bmc Public Health*. 2013; 13: 664. <https://doi.org/10.1186/1471-2458-13-664> PMID: 23866159
7. Li S, Yang H, Guo Y. Comparative efficacy and safety of urate-lowering therapy for the treatment of hyperuricemia a systematic review and network meta-analysis. *Scientific Reports*. 2016; 6:33082. <https://doi.org/10.1038/srep33082> PMID: 27605442
8. Sun H, Wang N, Chen C, Nie X, Han B, Li Q, et al. Cadmium exposure and its association with serum uric acid and hyperuricemia. *Scientific Reports*. 2017; 7(1):550. <https://doi.org/10.1038/s41598-017-00661-3> PMID: 28373703
9. Billiet L, Doaty S, Katz JD, Velasquez MT. Review of hyperuricemia as new marker for metabolic syndrome. *Isrn Rheumatology*. 2014;5–6: 852954. <https://doi.org/10.1155/2014/852954> PMID: 24693449
10. Ford ES, Li C, Cook S, Choi HK. Serum concentrations of uric acid and the metabolic syndrome among us children and adolescents. *Circulation*. 2007; 115(19):2526–32. <https://doi.org/10.1161/CIRCULATIONAHA.106.657627> PMID: 17470699
11. Zuo T, Liu X, Jiang L, Mao S, Yin X, Guo L. Hyperuricemia and coronary heart disease mortality: a meta-analysis of prospective cohort studies. *BMC Cardiovascular Disorders*. 2016; 16(1):207. <https://doi.org/10.1186/s12872-016-0379-z> PMID: 27793095
12. Kojima S, Matsui K, Ogawa H, Jinnouchi H, Hiramitsu S, Hayashi T, et al. Rationale, design, and baseline characteristics of a study to evaluate the effect of febuxostat in preventing cerebral, cardiovascular, and renal events in patients with hyperuricemia. *Journal of Cardiology*. 2017; 69(1): 169–175. <https://doi.org/10.1016/j.jjcc.2016.02.015> PMID: 27005768
13. Li L, Yang C, Zhao Y, Zeng X, Liu F, Fu P, et al. Is hyperuricemia an independent risk factor for new-onset chronic kidney disease?: a systematic review and meta-analysis based on observational cohort studies. *BMC Nephrology*. 2014; 15(1):122. <https://doi.org/10.1186/1471-2369-15-122> PMID: 25064611
14. Malik UZ, Hundley NJ, Romero G, Radi R, Freeman BA, Tarpey MM, et al. Febuxostat inhibition of endothelial-bound xo: implications for targeting vascular ros production. *Free Radical Biology & Medicine*. 2011; 51(1): 179–184. <https://doi.org/10.1016/j.freeradbiomed.2011.04.004> PMID: 21554948
15. Okamoto K, Eger BT, Nishino T, Kondo S, Pai EF, Nishino T, et al. An extremely potent inhibitor of xanthine oxidoreductase crystal structure of the enzyme-inhibitor complex and mechanism of inhibition. *Journal of Biological Chemistry*. 2003; 278(3): 1848–1855. <https://doi.org/10.1074/jbc.M208307200> PMID: 12421831

16. Stamp LK, Haslett J, Frampton C, White D, Gardner D, Stebbings S, et al. The safety and efficacy of benzbromarone in gout in aotearoa new zealand. *Internal Medicine Journal*. 2016; 46(9): 1075–1080. <https://doi.org/10.1111/imj.13173> PMID: 27391386
17. Robinson PC, Dalbeth N. Advances in pharmacotherapy for the treatment of gout. *Expert Opinion on Pharmacotherapy*. 2015; 16(4): 533–546. <https://doi.org/10.1517/14656566.2015.997213> PMID: 25547991
18. Kaufmann P, Török M, Hänni A, Gasser R, Krähenbühl S. Mechanisms of benzarone and benzbromarone-induced hepatic toxicity. *Hepatology*. 2005; 41(4):925–35. <https://doi.org/10.1002/hep.20634> PMID: 15799034
19. Calogiuri G, Nettis E, Di Leo E, Foti C, Ferrannini A, Butani L. Allopurinol hypersensitivity reactions: desensitization strategies and new therapeutic alternative molecules. *Inflammation & Allergy Drug Targets*. 2013; 12(1): 19–28. <https://doi.org/10.2174/1871528111312010004> PMID: 23092365
20. Li XX, Han M, Wang YY, Liu JP. Chinese herbal medicine for gout: a systematic review of randomized clinical trials. *Clinical Rheumatology*. 2013; 32(7): 943–959. <https://doi.org/10.1007/s10067-013-2274-7> PMID: 23666318
21. Multi-Disciplinary Expert Task Force on Hyperuricemia and Its Related Diseases. Chinese multi-disciplinary consensus on the diagnosis and treatment of hyperuricemia and its related diseases. *Zhonghua Nei Ke Za Zhi*. 2017; 56(3): 235–248. <https://doi.org/10.3760/cma.j.issn.0578-1426.2017.03.021> PMID: 28253612
22. Li LY, Lin ZJ, Zhang B, Wang XJ, Zhu CS, Niu HJ. Effect of Chinese herb chicory on renal organic anion transporter OAT3 -LIKE of hyperuricemia quails. *Tradit. Chin. Drug Res. Clin. Pharmacol.* 2015; 26(3): 284–289.
23. Zhou Q, Yu DH, Zhang C, Liu SM, Lu F. Total saponins from *Discorea nipponica* makino ameliorate urate excretion in hyperuricemic rats. *Planta Medica*. 2014; 80(15): 1259–1268. <https://doi.org/10.1055/s-0034-1383048> PMID: 25248048
24. Wang Y, Lin ZJ, Zhang B, Nie AZ, Bian M. *Cichorium intybus* promotes intestinal uric acid excretion by modulating *abcg2* in experimental hyperuricemia. *Nutrition & Metabolism*. 2017; 14(1): 38. <https://doi.org/10.1186/s12986-017-0190-6> PMID: 28630638
25. Jiang Y, Lin Y, Hu YJ, Song XJ, Pan HH, Zhang HJ. Caffeoylquinic acid derivatives rich extract from *gnaphalium pensylvanicum*, wild. ameliorates hyperuricemia and acute gouty arthritis in animal model. *BMC Complementary & Alternative Medicine*. 2017; 17(1): 320. <https://doi.org/10.1186/s12906-017-1834-9> PMID: 28623927
26. Ming H, Sha L, Hor T, Fan C, Ning W, Jihan H, et al. A network-based pharmacology study of the herb-induced liver injury potential of traditional hepatoprotective Chinese herbal medicines. *Molecules*. 2017; 22(4): 632. <https://doi.org/10.3390/molecules22040632> PMID: 28420096
27. Wang J, Ma Z, Niu M, Zhu Y, Liang Q, Zhao Y, et al. Evidence chain-based causality identification in herb-induced liver injury: exemplification of a well-known liver-restorative herb *polygonum multiflorum*. *Frontiers of Medicine*. 2015; 9(4): 457–467. <https://doi.org/10.1007/s11684-015-0417-8> PMID: 26459430
28. González-Terán B, Matesanz N, Nikolic I, Verdugo MA, Sreeramkumar V, Hernández-Cosido L, et al. P38 $\gamma$  and p38 $\delta$  reprogram liver metabolism by modulating neutrophil infiltration. *Embo Journal*. 2016; 35(5): 536–552. <https://doi.org/10.15252/embj.201591857> PMID: 26843485
29. Xiao Y, Wang J, Yan W, Zhou K, Cao Y, Cai W. P38 $\alpha$ ±MAPK antagonizing JNK to control the hepatic fat accumulation in pediatric patients onset intestinal failure. *Cell Death & Disease*. 2017; 8(10): e3110. <https://doi.org/10.1038/cddis.2017.523> PMID: 29022907
30. Justyna Godyń, Hebda M, Anna Więckowska, Krzysztof Więckowski, Malawska B, Bajda M. Lipophilic properties of anti-alzheimer's agents determined by micellar electrokinetic chromatography and reversed-phase thin-layer chromatography. *Electrophoresis*. 2017; 38(9–10):1268–1275. <https://doi.org/10.1002/elps.201600473> PMID: 28169440
31. Pathak A, Singour PK, Srivastava AK, Gouda P, Kumar S, Goutam BK. Hansch analysis of novel acetamide derivatives as highly potent and specific MAO-A inhibitors. *Cent Nerv Syst Agents Med Chem*. 2016; 16(2):143–51. <https://doi.org/10.2174/1871524916666151210143347> PMID: 26654229
32. Ru J, Li P, Wang J, Zhou W, Li B, Huang C, et al. TCMSP: a database of systems pharmacology for drug discovery from herbal medicines. *J Cheminformatics*. 2014; 6(1):13. <https://doi.org/10.1186/1758-2946-6-13> PMID: 24735618
33. Liu X, Ouyang S, Yu B, Liu Y, Huang K, Gong J, et al. PharmMapper server: a webserver for potential drug target identification using pharmacophore mapping approach. *Nucleic Acids Research*. 2010; 38 (Web-Server-Issue): 609–614. <https://doi.org/10.1093/nar/gkq300> PMID: 20430828
34. Huang J, Tang H, Cao S. Molecular targets and associated potential pathways of danlu capsules in hyperplasia of mammary glands based on systems pharmacology. *Evidence-Based Complementary and Alternative Medicine*. 2017; 2017(9):1–10. <https://doi.org/10.1155/2017/1930598> PMID: 28620417

35. Wang X, Shen Y, Wang S, Li S, Zhang W, Liu X, et al. PharmMapper 2017 update: a web server for potential drug target identification with a comprehensive target pharmacophore database. *Nucleic Acids Research*. 2017; 45(W1): W356–W360. <https://doi.org/10.1093/nar/gkx374> PMID: 28472422
36. The UniProt Consortium. UniProt: the universal protein knowledgebase. *Nucleic Acids Res*. 2017; 45(D1):D158–D169. <https://doi.org/10.1093/nar/gkw1099> PMID: 27899622
37. Hamosh A, Scott AF, Amberger JS, Bocchini CA, McKusick VA. Online mendelian inheritance in man (OMIM), a knowledgebase of human genes and genetic disorders. *Nucleic Acids Research*, 2005; 33(1):514–517. <https://doi.org/10.1093/nar/gki033> PMID: 15608251
38. Chen X, Ji ZL, Chen YZ. TTD: Therapeutic Target Database. *Nucleic Acids Res*. 2002; 30(1):412–415. <https://doi.org/10.1093/nar/30.1.412> PMID: 11752352
39. Barbarino JM, Whirl-Carrillo M, Altman RB, Klein TE. PharmGKB: a worldwide resource for pharmacogenomic information. *Wiley Interdisciplinary Reviews Systems Biology & Medicine*, 2018; 10(4):e1417. <https://doi.org/10.1002/wsbm.1417> PMID: 29474005
40. Becker KG, Barnes KC, Bright TJ, Wang SA. The genetic association database. *Nature Genetics*. 2004; 36(5):431–432. <https://doi.org/10.1038/ng0504-431> PMID: 15118671
41. Thornton CE, Makris A, Ogle RF, Toohar JM, Hennessy A. Bisogenet: a new tool for gene network building, visualization and analysis. *Bmc Bioinformatics*. 2010; 11(1):91. <https://doi.org/10.1186/1471-2105-11-91> PMID: 20163717
42. Kerrien S, Aranda B, Breuza L, Bridge A, Broackes-Carter F, Chen C, et al. The IntAct molecular interaction database in 2012. *Nucleic Acids Research*. 2012; 40(21):841–846. <https://doi.org/10.1093/nar/gkr1088> PMID: 22121220
43. Goel R, Muthusamy B, Pandey A, Prasad TSK. Human protein reference database and human proteinpedia as resources for phosphoproteome analysis. *Molecular Biosystems*. 2012; 8(2): 453–463. <https://doi.org/10.1039/c1mb05340j> PMID: 22159132
44. Ceol A, Chatr Aryamontri A, Licata L, Peluso D, Briganti L, Perfetto L, et al. Mint, the molecular interaction database: 2009 update. *Nucleic Acids Research*, 2007; 35(Database issue): 532–539. <https://doi.org/10.1093/nar/gkp983> PMID: 19897547
45. Xenarios I, Salwinski L, Duan XJ, Higney P, Kim SM, Eisenberg D. DIP, the Database of Interacting Proteins: a research tool for studying cellular networks of protein interactions. *Nucleic Acids Research*, 2002; 30(1):303–305. <https://doi.org/10.1093/nar/30.1.303> PMID: 11752321
46. Oughtred R, Chatr-aryamontri A, Breitkreutz BJ, Chang CS, Rust JM, Theesfeld CL, et al. BioGRID: A Resource for Studying Biological Interactions in Yeast. *Cold Spring Harbor Protocols*. 2016; 2016(1): pdb.top080754. <https://doi.org/10.1101/pdb.top080754> PMID: 26729913
47. Don Gilbert. Biomolecular Interaction Network Database. *Briefings in Bioinformatics*. 2005; 6(2):194–198. <https://doi.org/10.1093/bib/6.2.194> PMID: 15975228
48. Martin A, Ochagavia ME, Rabasa LC, et al. Bisogenet: a new tool for gene network building, visualization and analysis. *BMC Bioinformatics*. 2010; 11:11:91. <https://doi.org/10.1186/1471-2105-11-91>
49. Tang Y, Li M, Wang J, Pan Y, Wu FX. CytoNCA: a cytoscape plugin for centrality analysis and evaluation of protein interaction networks. *Biosystems*. 2015; 127:67–72. <https://doi.org/10.1016/j.biosystems.2014.11.005> PMID: 25451770
50. Boezio B, Audouze K, Ducrot P, Taboureau O. Network-based Approaches in Pharmacology. *Mol Inform*. 2017; 36(10). <https://doi.org/10.1002/minf.201700048> PMID: 28692140
51. Shannon P, Markiel A, Ozier O, Baliga NS, Wang JT, Ramage D, et al. Cytoscape: a software environment for integrated models of biomolecular interaction networks. *Genome Res*. 2003; 13(11):2498–2504. <https://doi.org/10.1101/gr.1239303> PMID: 14597658
52. Jiao X, Sherman BT, Huang da W, Stephens R, Baseler MW, Lane HC, et al. DAVID-WS: a stateful web service to facilitate gene/protein list analysis. *Bioinformatics*. 2012; 28(13):1805–1806. <https://doi.org/10.1093/bioinformatics/bts251> PMID: 22543366
53. Haw R1, Hermjakob H, D'Eustachio P, Stein L. Reactome Pathway Analysis to Enrich Biological Discovery in Proteomics Datasets. *Proteomics*. 2011; 11(18):3598–3613. <https://doi.org/10.1002/pmic.201100066> PMID: 21751369
54. Vilar S, Sobarzo-Sanchez E, Santana L, Uriarte E. Molecular Docking and Drug Discovery in  $\beta$ -Adrenergic Receptors. *Current Medicinal Chemistry*. 2017; 24(39): 4340–4359. <https://doi.org/10.2174/0929867324666170724101448> PMID: 28738772
55. Burley SK, Berman HM, Kleywegt GJ, Markley JL, Nakamura H, Velankar S. Protein Data Bank (PDB): The Single Global Macromolecular Structure Archive. *Methods Mol Biol*. 2017; 1607:627–641. [https://doi.org/10.1007/978-1-4939-7000-1\\_26](https://doi.org/10.1007/978-1-4939-7000-1_26) PMID: 28573592

56. Pettersen EF, Goddard TD, Huang CC, Couch GS, Greenblatt DM, Meng EC, et al. UCSF Chimera—A visualization system for exploratory research and analysis. *J Comput Chem*. 2004; 25(13):1605–1612. <https://doi.org/10.1002/jcc.20084> PMID: 15264254
57. Goddard TD, Huang CC, Ferrin TE. Software extensions to UCSF chimera for interactive visualization of large molecular assemblies. *Structure*. 2005; 13(3):473–482. <https://doi.org/10.1016/j.str.2005.01.006> PMID: 15766548
58. Morris GM, Huey R, Lindstrom W, Sanner MF, Belew RK, Goodsell DS, et al. AutoDock4 and AutoDock Tools4: Automated docking with selective receptor flexibility. *J Comput Chem*. 2009; 30(16):2785–2791. <https://doi.org/10.1002/jcc.21256> PMID: 19399780
59. Morris GM, Goodsell DS, Halliday RS, Huey R, Hart WE, Belew RK, et al. Automated docking using a Lamarckian genetic algorithm and an empirical binding free energy function. *J. Comp. Chem*. 1998; 19(14):1639–1662. [https://doi.org/10.1002/\(SICI\)1096-987X\(19981115\)19:143.0.CO;2-B](https://doi.org/10.1002/(SICI)1096-987X(19981115)19:143.0.CO;2-B)
60. Seeliger D, de Groot BL. Ligand docking and binding site analysis with PyMOL and Autodock/Vina. *J Comput Aided Mol Des*. 2010; 24(5):417–22. <https://doi.org/10.1007/s10822-010-9352-6> PMID: 20401516
61. Trott O, Olson AJ. AutoDock Vina: improving the speed and accuracy of docking with a new scoring function, efficient optimization, and multithreading. *J Comput Chem*. 2010; 31(2):455–461. <https://doi.org/10.1002/jcc.21334> PMID: 19499576
62. Rigsby RE, Parker AB. Using the PyMOL application to reinforce visual understanding of protein structure. *Biochem Mol Biol Educ*. 2016; 44(5):433–437. <https://doi.org/10.1002/bmb.20966> PMID: 27241834
63. Laskowski RA, Swindells MB. LigPlot+: Multiple Ligand–Protein Interaction Diagrams for Drug Discovery. *Journal of Chemical Information and Modeling*. 2011; 51(10):2778–2786. <https://doi.org/10.1021/ci200227u> PMID: 21919503
64. Mosmann T. Rapid colorimetric assay for cellular growth and survival: application to proliferation and cytotoxicity assays. *J Immunol Methods*. 1983; 65(1–2):55–63. PMID: 6606682
65. van Tonder A, Joubert AM, Cromarty AD. Limitations of the 3-(4,5-dimethylthiazol-2-yl)-2,5-diphenyl-2H-tetrazolium bromide (MTT) assay when compared to three commonly used cell enumeration assays. *BMC Res Notes*. 2015; 8(1):47. <https://doi.org/10.1186/s13104-015-1000-8> PMID: 25884200
66. González-Terán B, Matesanz N, Nikolic I, Verdugo MA, Sreeramkumar V, Hernández-Cosido L, et al. p38 $\gamma$  and p38 $\delta$  reprogram liver metabolism by modulating neutrophil infiltration. *EMBO J*. 2016; 35(5):536–552. <https://doi.org/10.15252/emj.201591857> PMID: 26843485
67. Xiao Y, Wang J, Yan W, Zhou K, Cao Y, Cai W. p38 $\alpha$  MAPK antagonizing JNK to control the hepatic fat accumulation in pediatric patients onset intestinal failure. *Cell Death Dis*. 2017; 8(10):e3110. <https://doi.org/10.1038/cddis.2017.523> PMID: 29022907
68. Sreekanth GP, Chuncharunee A, Sirimontaporn A, Panaampon J, Noisakran S, Yenchitsomanus PT, et al. SB203580 Modulates p38 MAPK Signaling and Dengue Virus-Induced Liver Injury by Reducing MAPKAPK2, HSP27, and ATF2 Phosphorylation. *PLoS One*. 2016; 11(2):e0149486. <https://doi.org/10.1371/journal.pone.0149486> PMID: 26901653
69. Qi XM, Miao LL, Cai Y, Gong LK, Ren J. ROS generated by CYP450, especially CYP2E1, mediate mitochondrial dysfunction induced by tetrandrine in rat hepatocytes. *Acta Pharmacol Sin*. 2013; 34(9):1229–1236. <https://doi.org/10.1038/aps.2013.62> PMID: 23892269
70. Zhang Z, Liu T, Yu M, Li K, Li W. The plant alkaloid tetrandrine inhibits metastasis via autophagy-dependent Wnt/ $\beta$ -catenin and metastatic tumor antigen 1 signaling in human liver cancer cells. *J Exp Clin Cancer Res*. 2018; 37(1):7. <https://doi.org/10.1186/s13046-018-0678-6> PMID: 29334999
71. Cai Q, Wei J, Zhao W, Shi S, Zhang Y, Wei R, et al. Toxicity of Evodiae fructus on rat liver mitochondria: the role of oxidative stress and mitochondrial permeability transition. *Molecules*. 2014; 19(12):21168–21182. <https://doi.org/10.3390/molecules191221168> PMID: 25521117
72. Wen B, Roongta V, Liu L, Moore DJ. Metabolic activation of the indoloquinazoline alkaloids evodiamine and rutaecarpine by human liver microsomes: dehydrogenation and inactivation of cytochrome P4503A4. *Drug Metab Dispos*. 2014; 42(6):1044–1054. <https://doi.org/10.1124/dmd.114.057414> PMID: 24696463
73. Lee Y, Kim YJ, Kim MH, Kwak JM. MAPK Cascades in Guard Cell Signal Transduction. *Front Plant Sci*. 2016; 7:80. <https://doi.org/10.3389/fpls.2016.00080> PMID: 26904052
74. Zhu JJ, Luo J, Wang W, Yu K, Wang HB, Shi HB, et al. Inhibition of FASN reduces the synthesis of medium-chain fatty acids in goat mammary gland. *Animal*. 2014; 8:1469–1478. <https://doi.org/10.1017/S1751731114001323> PMID: 24909980
75. Jiang Y, Yin X, Wu L, Qin Q, Xu J. MAPK/P53-mediated FASN expression in bone tumors. *Oncol Lett*. 2017; 13(6):4035–4038. <https://doi.org/10.3892/ol.2017.6015> PMID: 28588696

76. Xiao Y, Wang J, Yan W, Zhou K, Cao Y, Cai W. p38 $\alpha$  MAPK antagonizing JNK to control the hepatic fat accumulation in pediatric patients onset intestinal failure. *Cell Death Dis.* 2017; 8(10):e3110. <https://doi.org/10.1038/cddis.2017.523> PMID: 29022907
77. Chatterjee B, Wolff DW, Jothi M, Mal M, Mal AK. p38 $\alpha$  MAPK disables KMT1A-mediated repression of myogenic differentiation program. *Skelet Muscle.* 2016; 6:28. <https://doi.org/10.1186/s13395-016-0100-z> PMID: 27551368
78. Luo X, Fitzsimmons B, Mohan A, Zhang L, Terrando N, Kordasiewicz H, et al. Intrathecal administration of antisense oligonucleotide against p38 $\alpha$  but not p38 $\beta$  MAP kinase isoform reduces neuropathic and postoperative pain and TLR4-induced pain in male mice. *Brain Behav Immun.* 2018; 72:34–44. <https://doi.org/10.1016/j.bbi.2017.11.007> PMID: 29128611
79. Corre I, Paris F, Huot J. The p38 pathway, a major pleiotropic cascade that transduces stress and metastatic signals in endothelial cells. *Oncotarget.* 2017; 8(33):55684–55714. <https://doi.org/10.18632/oncotarget.18264> PMID: 28903453
80. Wang L, Huang QH, Li YX, Huang YF, Xie JH, Xu LQ, et al. Protective effects of silymarin on triptolide-induced acute hepatotoxicity in rats. *Mol Med Rep.* 2018; 17(1):789–800. <https://doi.org/10.3892/mmr.2017.7958> PMID: 29115625
81. Sato H, Tanaka T, Tanaka N. The effect of p38 mitogen-activated protein kinase activation on inflammatory liver damage following hemorrhagic shock in rats. *PLoS One.* 2012; 7(1):e30124. <https://doi.org/10.1371/journal.pone.0030124> PMID: 22253904
82. Dai C, Li D, Gong L, Xiao X, Tang S. Curcumin ameliorates furazolidone-induced DNA damage and apoptosis in human hepatocyte L02 cells by inhibiting ROS production and mitochondrial pathway. *Molecules.* 2016; 21(8):pii: E1061. <https://doi.org/10.3390/molecules21081061> PMID: 27556439
83. Hu Y, Wang S, Wang A, Lin L, Chen M, Wang Y. Antioxidant and hepatoprotective effect of Penthorum chinense Pursh extract against t-BHP-induced liver damage in L02 cells. *Molecules.* 2015; 20(4):6443–6453. <https://doi.org/10.3390/molecules20046443> PMID: 25867829
84. McGill MR. The past and present of serum aminotransferases and the future of liver injury biomarkers. *EXCLI J.* 2016; 15:817–828. <https://doi.org/10.17179/excli2016-800> PMID: 28337112
85. Senior JR. Alanine aminotransferase: a clinical and regulatory tool for detecting liver injury—past, present, and future. *Clin Pharmacol Ther.* 2012; 92(3):332–339. <https://doi.org/10.1038/clpt.2012.108> PMID: 22871997
86. Chen MF, Huang CC, Liu PS, Chen CH, Shiu LY. Saikosaponin a and saikosaponin d inhibit proliferation and migratory activity of rat HSC-T6 cells. *J Med Food.* 2013; 16(9):793–800. <https://doi.org/10.1089/jmf.2013.2762> PMID: 24044489
87. Meng A, Zhang X, Wu S, Wu M, Li J, Yan X, et al. In vitro modeling of COPD inflammation and limitation of p38 inhibitor—SB203580. *Int J Chron Obstruct Pulmon Dis.* 2016; 11:909–917. <https://doi.org/10.2147/COPD.S99810> PMID: 27199554
88. Su J, Cui X, Li Y, Mani H, Ferreyra GA, Danner RL, et al. SB203580, a p38 inhibitor, improved cardiac function but worsened lung injury and survival during *Escherichia coli* pneumonia in mice. *J Trauma.* 2010; 68(6):1317–1327. <https://doi.org/10.1097/TA.0b013e3181bb9cd3> PMID: 20068480
89. Yang ZH, Wu BL, Ye C, Jia S, Yang XJ, Hou R, et al. Targeting p38 pathway regulates bony formation via MSC recruitment during mandibular distraction osteogenesis in Rats. *Int J Med Sci.* 2016; 13(10):783–789. <https://doi.org/10.7150/ijms.16663> PMID: 27766028
90. Korashy HM, Anwar-Mohamed A, Soshilov AA, Denison MS, El-Kadi AO. The p38 MAPK inhibitor SB203580 induces cytochrome P4501A1 gene expression in murine and human hepatoma cell lines through ligand-dependent aryl hydrocarbon receptor activation. *Chem Res Toxicol.* 2011; 24(9):1540–8. <https://doi.org/10.1021/tx200141p> PMID: 21732638